Analysis of the Molecular Interaction of the Farnesyl Moiety of Transducin through the Use of a Photoreactive Farnesyl Analogue†

Ken'ichi Hagiwara,‡,§,|| Akimori Wada,⊥ Maiko Katadae,‡ Masayoshi Ito,⊥ Yoshikazu Ohya,@ Patrick J. Casey,# and Yoshitaka Fukada*,‡,§

Department of Biophysics and Biochemistry, Graduate School of Science, The University of Tokyo, Hongo, Bunkyo-ku, Tokyo 113-0032, Japan, Department of Integrated Biosciences, Graduate School of Frontier Sciences, The University of Tokyo, Kashiwanoha, Kashiwa, Chiba 277-8562, Japan, Japan Science and Technology Corporation, CREST, Tokyo, Japan, Department of Analytical Chemistry, Kobe Pharmaceutical University, Higashinada-ku, Kobe, Hyogo 658-8558, Japan, and Department of Pharmacology and Cancer Biology, Duke University Medical Center, Durham, North Carolina 27710-3813

Received July 3, 2003; Revised Manuscript Received October 18, 2003

ABSTRACT: Farnesylation of the γ-subunit of the retinal G-protein, transducin (Tα/T$\beta\gamma$), is indispensable for light-initiated signaling in photoreceptor cells. However, the farnesyl-mediated molecular interactions important for signaling are not well understood. To explore this issue, we created a functional T$\beta\gamma$ analogue in which the farnesyl group was replaced with a (3-azidophenoxy)geranyl (POG) group, a novel farnesyl analogue with a distal photoreactive azido group. In the presence of lipid membranes and/or Tα-GDP, UV irradiation of POG-modified T$\beta\gamma$ (POG-T$\beta\gamma$) invariably yielded a cross-linked product Tγ−Tβ, reflecting a constitutive interaction of the Tγ C-terminal lipid with Tβ. In addition to the Tγ−Tβ adduct, a Tγ−Tα cross-link was detected in the aqueous fraction. Reconstitution of POG-T$\beta\gamma$ with Tα and light-activated rhodopsin (Rh*) in photoreceptor membranes resulted in cross-linking of Tγ with a glycerophospholipid, indicating molecular interaction of the farnesyl group with cellular membranes. The Tγ−phospholipid cross-link was observed only in the presence of both Tα-GDP and Rh*, and was abolished by the addition of GTPγS or by replacing Rh* with opsin. These findings suggest a transient farnesyl−membrane interaction occurs only in a signaling state formed in a transducin−Rh* ternary complex. On the other hand, UV irradiation of POG-T$\beta\gamma$ in a soluble complex with phosducin, a negative regulator of G-protein, yielded a Tγ−phosducin adduct in addition to the Tγ−Tβ cross-link. These results illustrate that, rather than being a static membrane anchor, the farnesyl moiety plays an active role in the dynamics of protein−protein and protein−membrane interactions at defined steps in the signal transduction process.

Heterotrimeric guanine nucleotide-binding regulatory proteins (G-proteins) are composed of a guanine nucleotide-binding α-subunit (Gα) and a tight complex of β- and γ-subunits (G$\beta\gamma$). G-Proteins transduce extracellular signals captured by a variety of G-protein-coupled receptors (reviewed in refs *1* and *2*). Transducin (consisting of Tα[1] and T$\beta\gamma$), a member of the G-protein family, plays a pivotal role in the light-initiated signal transduction in retinal photoreceptor cells. Tα in the GDP-bound form (abbreviated Tα-GDP) and T$\beta\gamma$ both associate with metarhodopsin II, an active photoactivated intermediate of rhodopsin (*3*) (termed Rh* in this paper), to form a transient ternary complex. In this state, Rh* facilitates the exchange of GDP bound to Tα for cytosolic GTP, resulting in dissociation of the ternary complex into Tα-GTP, T$\beta\gamma$, and Rh*. A single molecule of Rh* catalyzes the formation of several hundred molecules of Tα-GTP, which in turn activates the effector enzyme cGMP-phosphodiesterase (PDE); the resulting decrease in the level of cGMP leads to a closure of cGMP-gated cation channels of the photoreceptor cells and hyperpolarization of the membrane potential. This visual transduction process is regulated by multiple additional regulatory proteins involved in quenching and/or desensitization of the cellular excitation. Phosducin is a 32 kDa protein expressed in the photoreceptor cells and in other tissues, and it is subject to phosphorylation at Ser^{73} by protein kinase A in the dark-adapted retina (*4*, *5*). Unphosphorylated phosducin forms a 1:1 complex with T$\beta\gamma$ (*6*), thereby sequestering T$\beta\gamma$ in the cytosol and thus inhibiting the signal amplification by decreasing the amount of T$\beta\gamma$ available in the membrane.

† This work was supported in part by Special Coordination Funds for Promoting Science and Technology and by Grants-in-Aid from the Ministry of Education, Culture, Sports, Science and Technology, the Japanese Government (to Y.F.), by a Human Frontiers Science Program grant (to Y.F.), and by NIH Grant GM46372 (to P.J.C.).

* To whom correspondence should be addressed. Telephone and Fax: +81 3 5802 8871. E-mail: sfukada@mail.ecc.u-tokyo.ac.jp.

‡ Department of Biophysics and Biochemistry, Graduate School of Science, The University of Tokyo.

§ Japan Science and Technology Corporation, CREST.

|| Present address: Department of Biochemistry and Cell Biology, National Institute of Infectious Diseases, Shinjuku-ku, Tokyo, Japan.

⊥ Kobe Pharmaceutical University.

@ Department of Integrated Biosciences, Graduate School of Frontier Sciences, The University of Tokyo.

Duke University Medical Center.

[1] Abbreviations: Tα, Tβ, and Tγ, α-, β-, and γ-subunits of transducin, respectively; Rh*, metarhodopsin II; FTase, farnesyltransferase; CPY, carboxypeptidase Y; POG-PP, (3-azidophenoxy)geranyl pyrophosphate; DATFP-GPP, (2-diazo-3,3,3-trifluoropropionyloxy)-geranyl pyrophosphate; ROS, rod outer segment; CBB, Coomassie Brilliant Blue R-250.

10.1021/bi0351514 CCC: $27.50
Published on Web 12/20/2003

In 1990, we and others found that Tγ was farnesylated at its carboxyl-terminal (C-terminal) cysteine residue through a thioether bond (*7*, *8*). It is now established that all the G-protein γ-subunits (of which 12 subtypes have been identified) share a C-terminal consensus sequence for isoprenylation, designated the CaaX motif where C, a, and X represent cysteine, aliphatic, and C-terminal amino acids, respectively (*9*). The X residue is a major determinant for which isoprenyl group, farnesyl or geranylgeranyl, is to be attached to the cysteine residue. Proteins are recognized by protein farnesyltransferase (FTase) when X is serine, methionine, glutamine, or alanine, whereas leucine at this position leads to the modification by protein geranylgeranyltransferase type I. According to their C-terminal sequence, Tγ (also known as γ1), γ8 (cone), and γ11 are farnesylated, while the other γ-subunits are geranylgeranylated (*10*). Following isoprenylation, the C-terminal aaX residues are removed by a specific endoprotease (*9*, *11*−*13*) and the newly exposed C-terminal prenylcysteine residue is subject to methylation (*7*, *9*, *10*, *14*).

Our previous studies showed that the farnesylation of Tγ is required for the functional interaction of T$\beta\gamma$ with Tα and for the effective coupling of transducin (Tα/T$\beta\gamma$) with Rh* (*7*, *15*−*19*). For example, T$\beta\gamma$ containing a Tγ truncated at the C-terminus (*7*, *15*−*17*) or recombinant T$\beta\gamma$ lacking the farnesyl group (*19*) was completely unable to support the GDP−GTP exchange reaction on Tα catalyzed by Rh*. In addition, artificial geranylgeranylation of Tγ increased the affinity of T$\beta\gamma$ not only for membranes but also for Tα and effectors such as adenylyl cyclase and phospholipase C (*19*). These observations have prompted us and others to speculate that the farnesyl linked to Tγ is not a simple membrane anchor but plays a more direct role in facilitating the protein−protein interactions (*7*, *15*−*19*; reviewed in refs *9*, *10*, *20*, and *21*). Hence, it appears that the attached farnesyl can promote membrane association on one hand and facilitate protein−protein interactions on the other.

Three-dimensional structures of G-proteins free from membranes have been determined by X-ray crystallography (*22*−*26*), but most of the studies employed engineered proteins lacking the prenyl group. Upon considering experimental difficulties in obtaining structural information on the prenyl group in membrane-associated G-protein, we have developed a novel photoreactive farnesyl analogue capable of monitoring the local environment around the distal tip of the lipid linked to Tγ. This study provides the first direct evidence of the dynamic interaction of the modifying lipid with particular molecules in the various signaling states of the G-protein.

EXPERIMENTAL PROCEDURES

Materials. Anti-bovine Tγ antibody was raised in our laboratory (*19*) or purchased (sc-373) from Santa Cruz Biotechnology, Inc. (Santa Cruz, CA). Anti-rhodopsin antiserum (*27*) was raised in our laboratory. Anti-Tα (sc-389) and anti-Gβ (sc-261) antibodies were purchased from Santa Cruz Biotechnology, Inc. Anti-phosducin antiserum was a kind gift from N. Miki (Osaka University Medical School, Osaka, Japan). Phospholipase A_2 (PLA_2, *Apis mellifera*) and sphingomyelinase (SMase, *Bacillus cereus*) were from Sigma. Carboxypeptidase Y (CPY) was from Peptide Institute, Inc. (Osaka, Japan), and [^{35}S]GTPγS was from NEN DuPont. Cytochrome *c* was from Sigma (c-7752).

Synthesis of (3-Azidophenoxy)geranyl Pyrophosphate and (2-Diazo-3,3,3-trifluoropropionyloxy)geranyl Pyrophosphate. For the synthesis of (3-azidophenoxy)geranyl pyrophosphate (POG-PP), geraniol was chloroacetylated and subsequently oxidized to give 1-chloroacetoxy-3,7-dimethyl-8-hydroxy-2,6-octadiene (hydroxygeranyl chloroacetate) (*28*). The hydroxyl group was then chlorinated with *N*-chlorosuccinimide and dimethyl sulfide to yield the chlorogeranyl chloroacetate (*29*). 3-Aminophenol was converted by diazotization with $NaNO_2$ and HCl followed by the reaction with NaN_3 to 3-azidophenol, which was purified by column chromatography on a silica gel with benzene and ethyl acetate (stepwise elution from 10/0 to 8/2, v/v). The TLC R_f equaled 0.82 [on a silica gel 60 HPTLC plate from Merck, 8/2 (v/v) benzene/ethyl acetate mixture]. 3-Azidophenol (1 mmol) was mixed successively with 0.5 mmol of EtONa (in EtOH) and 0.4 mmol of chlorogeranyl chloroacetate, and the resulting mixture was stirred at 23 °C for 2 h to afford the azidophenoxy ether. After removal of the chloroacetyl group by the addition of 200 μL of a 9/1 (v/v) MeOH/28% ammonium hydroxide mixture, (3-azidophenoxy)geraniol was purified by column chromatography on a silica gel with CH_2Cl_2 and MeOH (stepwise elution from 10/0 to 2/1, v/v). The R_f of the compound on silica gel TLC developed with benzene and ethyl acetate (8/2, v/v) equaled 0.55. The ^{1}H NMR chemical shifts (δ, parts per million) in [^{2}H]chloroform were as follows: 1.70 (3H, s), 1.75 (3H, s), 2.15 (2H, t), 2.25 (2H, m), 4.18 (2H, d), 4.40 (2H, s), 5.45 (1H, t), 5.55 (1H, t), 6.60 (1H, s), 6.65 (1H, d), 6.75 (1H, d), and 7.25 (1H, m). (3-Azidophenoxy)geraniol was chlorinated and pyrophosphorylated according to the previously reported method (*29*) to give (3-azidophenoxy)geranyl pyrophosphate (POG-PP) ammonium salt. The R_f of the compound on the silica gel TLC developed with a 6/1/3 (v/v/v) isopropanol/H_2O/28% ammonium hydroxide mixture equaled 0.31.

(2-Diazo-3,3,3-trifluoropropionyloxy)geranyl pyrophosphate (DATFP-GPP) was also synthesized from geraniol. DATFP-GPP was first synthesized by Baba and Allen (*28*), who adopted the esterification of hydroxygeranyl chloroacetate with 2-diazo-3,3,3-trifluoropropionyl chloride; in their procedure, the compound was prepared from 2,2,2-trifluorodiazoethane with phosgene, an extremely toxic gas. We have developed a convenient method for the esterification of hydroxygeranyl *tert*-butyldimethylsilyl ether using 2-diazo-3,3,3-trifluoropropionate, which was readily prepared from the reaction of ethyl trifluoropyruvate with tosylhydrazide and subsequent treatment with $POCl_3$ in pyridine (*30*). Thus, geraniol was converted to the 1-*tert*-butyldimethylsilyl-3,7-dimethyl-8-hydroxy-2,6-octadiene by the protection of hydroxy group with *tert*-butyldimethylsilyl (TBS) chloride, and subsequent hydroxylation. Esterification easily proceeded by treatment with the lithium salt of 1-*tert*-butyldimethylsilyl-3,7-dimethyl-8-hydroxy-2,6-octadiene and ethyl 2-diazo-3,3,3-trifluoropropionate in tetrahydrofuran at 0 °C to produce the silylated ester. Deprotection of the TBS group was achieved with tetrabutylammonium fluoride in tetrahydrofuran at 0 °C to give the (2-diazo-3,3,3-trifluoropropionyloxy)geraniol. The ^{1}H NMR chemical shifts (δ, parts per million) in [^{2}H]chloroform were as follows: 1.65 (3H, s), 1.67 (3H, s), 2.07 (2H, t), 2.18 (2H, m), 4.14 (2H, d), 4.63

(2H, s), 5.39 (1H, t), 5.45 (1H, t), and 7.25 (1H, m). The (2-diazo-3,3,3-trifluoropropionyloxy)geraniol so produced was then subjected to chlorination and pyrophosphorylation (*29*) to give DATFP-GPP.

Preparation of Recombinant Tβγ and Its POG- or DATFP-Geranyl Modification. The recombinant Tβγ complex containing Tγ with an unmodified C-terminal structure (Pro^2-Ser^{74}; termed Tγ-VIS) was prepared in *Trichoplusia ni* (Tn5) insect cells using a baculovirus expression system (*19*); the unmodified form of Tβγ (Tβγ-VIS) was purified as described previously (*10*, *19*). Recombinant yeast FTase was expressed in *Escherichia coli* DH5α by cotransfection with the pBH57 and pMM101-3 plasmids encoding the α- and β-subunits, respectively (*31*). Recombinant yeast FTase was purified from the soluble fraction of the DH5α cell lysate according to the method described previously (*31*−*33*). For the POG transfer reaction, Tβγ-VIS (final concentration of 40 μg/mL) was incubated at 37 °C for 90 min with both 0.6 μmol of POG-PP and recombinant FTase (final concentration of 1 μg/mL) in a total of 12.5 mL of 10 mM Tris-HCl (pH 7.6), 2 mM $MgCl_2$, 0.1 mM phenylmethanesulfonyl fluoride (PMSF), 1 μg/mL E-64, 1 mM mercaptoethanol, and 5 μM $ZnCl_2$. The C-terminal aaX sequence (Val^{72}-Ile^{73}-Ser^{74}) of Tγ was cleaved by incubation of POG-Tβγ-VIS with carboxypeptidase Y (CPY; see Results). After the CPY treatment, POG-Tβγ was purified with a MonoQ HR 5/5 column (Pharmacia) with a linear gradient from 0 to 0.5 M NaCl in 24 mL of 10 mM Tris-HCl (pH 7.6), 0.1 mM PMSF, 2 mM $MgCl_2$, 1 μg/mL E-64, and 1 mM mercaptoethanol at a flow rate of 0.8 mL/min. The completion of these modifications at the C-terminus of Tγ was verified by subjecting 100 μL aliquots of the reaction mixture to HPLC analysis using an ODS column (Cosmosil $5C_{18}$-P300, 4.6 mm × 150 mm, Nacalai tesque, Kyoto, Japan) with a 50 mL linear gradient elution from a 70/30/0.05 (v/v/v) H_2O/CH_3CN/CF_3COOH solvent to the same solvent at a 20/80/0.05 (v/v/v) ratio at a flow rate of 1.0 mL/min (*10*, *19*, *34*). Mass spectometric analysis of the modified Tγ was carried out using a Voyager-DE MALDI-TOF spectrometer (Applied Biosystems, Foster City, CA). DATFP-geranylated Tβγ was prepared in a similar fashion using recombinant FTase and DATFP-GPP as the prenyl donor.

Preparation of Liposomes and Rod Outer Segment Membranes. Multilamellar liposomes composed of dipalmitoylphosphatidylcholine, 1-palmitoyl-2-oleoylphosphatidylcholine, and cholesterol in a 4/4/2 molar ratio were prepared as described previously (*35*). Rod outer segment (ROS) membranes were prepared from dark-adapted bovine retinas (*34*), and the amount of rhodopsin in the membrane was determined spectrophotometrically (*34*). Transducin-depleted ROS membranes were prepared in the dark by washing ROS membranes seven times with 5 mM Tris-HCl (pH 7.2), 0.5 mM $MgCl_2$, 1 mM DTT, 0.1 mM PMSF, 4 μg/mL aprotinin, and 4 μg/mL leupeptin containing 100 μM GTP, then three times with the same buffer containing 10 μM GTPγS, and finally five times with the buffer alone. Opsin membranes, in which rhodopsin was converted to inactive opsin and retinal oxime, were prepared as described previously (*34*).

Preparation of Retinal Transducin Subunits and Recombinant Phosducin. Retinal transducin subunits (Tα and Tβγ) were purified from dark-adapted bovine retina according to the method described previously (*15*, *34*). The obtained Tβγ fraction contained two chemically distinct forms of farnesylated Tγ, i.e., the carboxyl-methylated form at its C-terminus and the nonmethylated form (*15*, *34*), and the two subspecies of the Tβγ complex were further separated with a Superdex 75 pg column (HiLoad 26/60, Pharmacia) equipped with a fast protein liquid chromatography (FPLC) system (*34*). Proteins were eluted with 10 mM MOPS-NaOH (pH 7.4), 0.1 M NaCl, 2 mM $MgCl_2$, 1 mM mercaptoethanol, 0.1 mM PMSF, and 0.2 mg/mL soybean trypsin inhibitor. The farnesylated but not methylated form of retinal Tβγ obtained by FPLC (designated retinal Tβγ) was used in the study presented here. Rat phosducin cDNA (American Type Culture Collection, ATCC 63147) was cloned into pET3a (Novagen) after PCR amplification with a pair of primers, 5′-GGAAT TCATA TGGAA GAAGC CGCAA GC-3′ and 5′-CGCGG ATCCT TATTA CTCGA TATCT TCATC-3′. Recombinant phosducin was expressed in *E. coli* BL21DE3-(pLysS) cells and purified from the soluble fraction of the cell lysate by chromatography on DEAE-Sepharose, Phenyl-Sepharose, HiTrap-Q, and Sephadex G-100 in that order.

Photoaffinity Experiments. Photoaffinity labeling experiments were performed in 10 mM MOPS-NaOH (pH 7.4), 0.1 M NaCl, 2 mM $MgCl_2$, 1 mM mercaptoethanol, 0.1 mM PMSF, and 0.2 mg/mL soybean trypsin inhibitor. The samples (usually 170 μL) were placed on ice 4 cm from a 20 W suntan light with an illuminating spectrum at ∼300 nm, and three cycles of irradiation (40 s each) were applied at 60 s intervals. Following UV irradiation, the samples containing the liposomes or ROS membranes were centrifuged at 12000*g* for 20 min at 4 °C to separate the supernatant from the membrane fraction. For rhodopsin activation, transducin-depleted ROS membranes were irradiated with an orange light (>540 nm) for 1 min at 4 °C (*34*), and then mixed with POG-Tβγ and/or Tα prior to UV irradiation. After UV irradiation, the samples were subjected to SDS−PAGE (*36*) for Western blotting and CBB staining. Positive signals in the Western blots were detected by Renaissance (PerkinElmer Life Science) or CDP-Star chemiluminescent reagents (New England Biolabs) with the aid of Hyperfilm-ECL films (Amersham Pharmacia Biotech). If the blots were to be reprobed, they were first washed in 62.5 mM Tris-HCl (pH 6.8), 2% (w/v) SDS, and 0.78% (v/v) mercaptoethanol at 50 °C for 30 min. For better resolution of the cross-linked products, a modified SDS−PAGE method (*37*) was employed in which the concentrations of the gel buffer and running buffer were raised to twice that of Laemmli's protocol (*36*).

RESULTS

Preparation of POG-Tβγ and Assessment of Its Ability To Support G-Protein Function. The unmodified recombinant Tβγ complex was recovered from the cytosolic fraction of the insect cells expressing Tβ and Tγ (*10*, *19*). Tγ in this complex had the nascent C-terminal structure (Cys^{71}-Val^{72}-Ile^{73}-Ser^{74}, designated Tγ-VIS) and a processed N-terminus (Pro^2 as in native retinal Tγ). This form of the Tβγ complex (Tβγ-VIS) was purified and used as a substrate for transferring the photoreactive farnesyl analogue POG-PP (Figure 1) to Tγ. In the reaction catalyzed by yeast FTase, the rate of transfer of POG to Tγ was indistinguishable from that of farnesyl transfer under the conditions employed (Figure 2A), indicating appropriate accommodation of POG in the far-

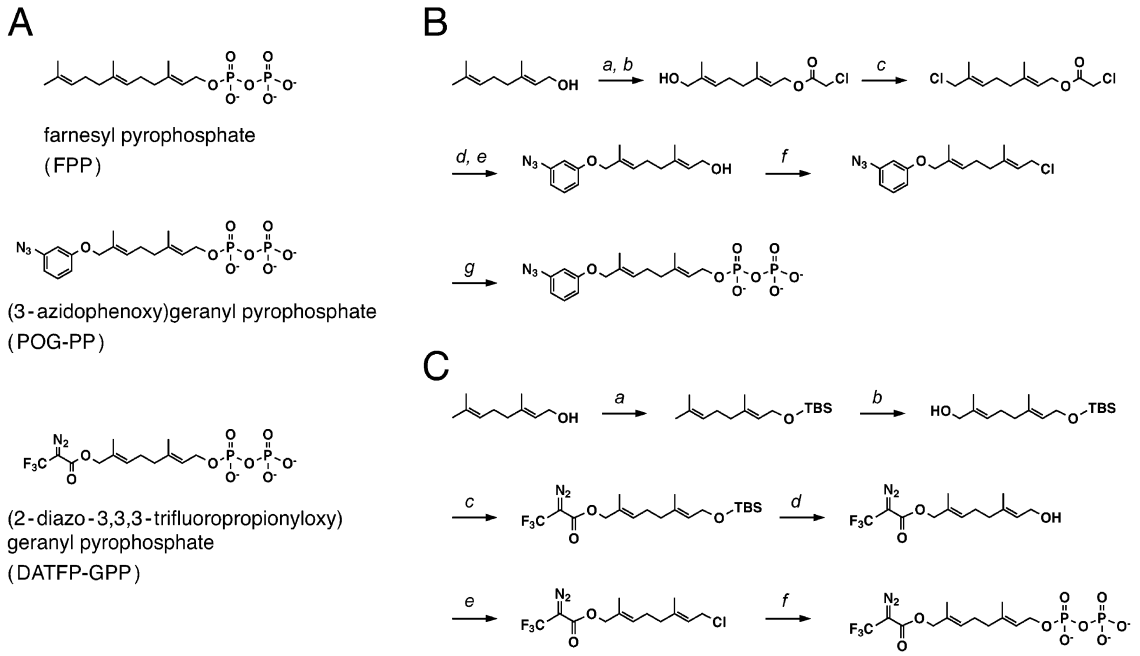

FIGURE 1: (3-Azidophenoxy)geranyl pyrophosphate (POG-PP) and (2-diazo-3,3,3-trifluoropropionyloxy)geranyl pyrophosphate (DATFP-GPP) as the analogues of farnesyl pyrophosphate. (A) Structures of farnesyl pyrophosphate, POG-PP, and DATFP-GPP. (B) Synthesis of POG-PP: (*a*) chloroacetyl chloride, (*b*) selenious acid and *tert*-butyl hydroperoxide, (*c*) *N*-chlorosuccinimide and dimethyl sulfide, (*d*) 3-azidophenol and sodium ethoxide, (*e*) 28% ammonium hydroxide, (*f*) *N*-chlorosuccinimide and dimethyl sulfide, and (*g*) tetrabutylammonium pyrophosphate. (C) Synthesis of DATFP-GPP: (*a*) *tert*-butyldimethylsilyl chloride (TBS-Cl), triethylamine, (4-dimethylamino)pyridine, and methylene chloride, (*b*) selenious acid and *tert*-butyl hydroperoxide, (*c*) *n*-BuLi and ethyl 3,3,3-trifluoro-2-diazopropionate, (*d*) tetrabutylammonium fluoride, (*e*) *N*-chlorosuccinimide and dimethyl sulfide, and (*f*) tetrabutylammonium pyrophosphate.

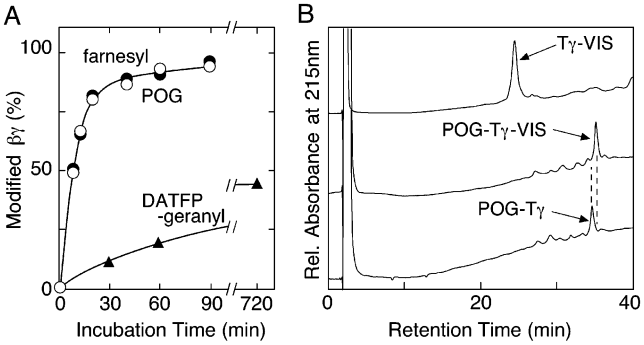

FIGURE 2: Transfer of farnesyl analogues to T$\beta\gamma$. (A) Time courses of prenyl transfer reactions catalyzed by yeast FTase. Unmodified T$\beta\gamma$-VIS was incubated with yeast FTase in the presence of POG-PP (●), DATFP-GPP (▲), or farnesyl pyrophosphate (○) at 37 °C, and aliquots of the reaction mixtures were subjected to HPLC analysis to estimate the amount of the product from the peak areas of POG-Tγ-VIS (●), DATFP-geranyl-Tγ-VIS (▲), or farnesyl-Tγ-VIS (○). (B) Reverse phase HPLC chromatograms of samples before (top trace) and after (middle trace) the POG transfer reaction, which was followed by the CPY treatment (bottom trace). HPLC analysis was performed as described in Experimental Procedures. Each peak fraction detected by the absorbance at 215 nm was collected and analyzed by MALDI-TOF mass spectrometry with a Voyager-DE (Applied Biosystems) spectrometer. The singly and doubly protonated ion signals of cytochrome *c* (horse heart, M_r = 12 359.7) were used as the internal standard of mass calibration. The observed $[M + H]^+$ values of the peak fractions were 8412.0 (top), 8682.1 (middle), and 8382.6 (bottom), in good agreement with the calculated $[M + H]^+$ values of Tγ-VIS (8411.4), POG-Tγ-VIS (8680.8), and POG-Tγ (8381.4), respectively. Due to adsorption, Tβ was not eluted from the column (*17*).

nesyl-binding pocket in the FTase catalytic site. The POG-modified form of Tγ-VIS (termed POG-Tγ-VIS) was then subjected to the C-terminal proteolysis by incubating the reaction mixture at 37 °C for 2.5 h with CPY as described in Experimental Procedures. The completion of each reaction was confirmed by reverse phase HPLC (*10*, *19*, *34*) and mass spectrometry, in which a peak containing Tγ-VIS (Figure 2B, top) shifted to a peak of POG-Tγ-VIS with a longer retention time (Figure 2B, middle), and subsequently to a peak of POG-Tγ upon the CPY treatment (Figure 2B, bottom). The POG-modified cysteine was completely resistant to CPY digestion. Peptide mapping analysis (*18*) demonstrated that the C-terminus of Tβ remained intact after CPY treatment, and the N-terminal Ser^2 was N-acetylated (data not shown) as was previously observed for bovine retinal Tβ (*18*).

The purified preparation of POG-T$\beta\gamma$ exhibited T$\beta\gamma$ activity similar to or slightly lower than that of bovine retina-derived T$\beta\gamma$ (described as 'retinal T$\beta\gamma$' hereafter; see Experimental Procedures) in stimulating the binding of GTPγS to Tα in the presence of a photoactivated intermediate of rhodopsin (termed Rh*) (Figure 3). On the other hand, essentially no activity was detected using the preparation prior to the POG transfer reaction (i.e., containing unprenylated T$\beta\gamma$-VIS) (Figure 3), indicating that the POG moiety can functionally substitute for the farnesyl that is indispensable for the receptor-mediated G-protein activation (*7*, *19*).

We also prepared another type of photoreactive T$\beta\gamma$, DATFP-geranylated T$\beta\gamma$, in a manner similar to that described for POG-T$\beta\gamma$ (Figure 1). The enzymatic transfer reaction of DATFP-GPP to recombinant T$\beta\gamma$-VIS was much slower than that of POG-PP (Figure 2A), and typically no more than 40−50% of T$\beta\gamma$-VIS was modified with DATFP-GPP even after incubation at 37 °C for 12 h. Such a prolonged incubation gave rise to background (UV irradiation-independent) cross-linked products, possibly due to a thermal reaction of the reactive diazo group. However,

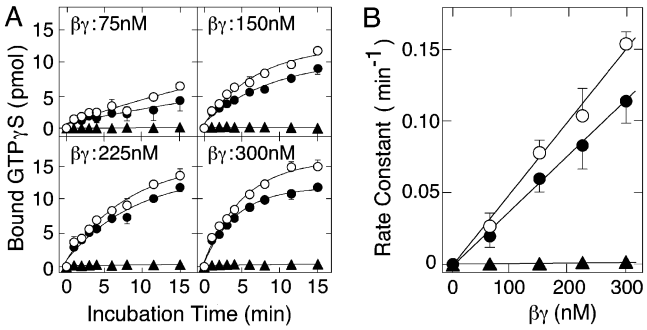

FIGURE 3: Rh*-catalyzed binding of GTPγS to Tα stimulated by POG-T$\beta\gamma$. (A) Time courses of binding of GTPγS to Tα in the presence of various concentrations of POG-T$\beta\gamma$ (●), retinal T$\beta\gamma$ (○), and unmodified T$\beta\gamma$-VIS (▲). Each reaction was carried out (*34*) in a set of duplicate mixtures (each 100 μL) composed of various concentrations of POG-T$\beta\gamma$ or retinal T$\beta\gamma$ (75, 150, 225, and 300 nM), 0.8 μM retinal Tα, 30 nM metarhodopsin II (Rh*) in ROS membranes, 0.002% Lubrol PX, 2.5 mg/mL ovalbumin, and 10 μM [^{35}S]GTPγS (74 MBq/mmol) in 10 mM MOPS-NaOH buffer (pH 7.5) containing 1 mM $MgCl_2$. The reaction was initiated by the addition of [^{35}S]GTPγS, and at the indicated times of incubation at 0 °C, 10 μL aliquots were transferred to multi Screen filter cups (Millipore, 0.45 μm cellulose membrane) filled with 170 μL of 100 mM Tris-HCl (pH 7.5, at 0 °C) containing 1 mM $MgCl_2$ and 2 mM GTP to quench GTPγS binding. Filters were washed four times, and the radioactivity was determined by a liquid scintillation method as described previously (*19*, *34*). The data were fitted to the equation $B(t) = B_{max}[1 - \exp(-kt)]$, where $B(t)$ is the amount of bound GTPγS at time t (minutes) and B_{max} (in picomoles) is the maximum binding at infinite time (*19*, *34*). (B) The rate constants (k) calculated from panel A were plotted against the concentrations of POG-T$\beta\gamma$ (●), retinal T$\beta\gamma$ (○), and unmodified T$\beta\gamma$-VIS (▲).

DATFP-geranylated T$\beta\gamma$ yielded the UV irradiation-induced cross-linked signals (see the Supporting Information) that were almost indistinguishable from those with POG-T$\beta\gamma$ (see below). We therefore describe in this paper only the results of photoaffinity labeling obtained from the use of POG-T$\beta\gamma$.

Photoaffinity Labeling of POG-T$\beta\gamma$ in the Absence of Rhodopsin. POG-T$\beta\gamma$ was subjected to UV irradiation in solution (Figure 4, lanes 1−4), and the product was immunoblotted with anti-Tγ antibody that detected a band of 43 kDa in addition to free Tγ (Figure 4A, lane 3). This 43 kDa band was not detected in UV-irradiated retinal T$\beta\gamma$ (lane 1) or in POG-T$\beta\gamma$ prior to UV irradiation (lane 2), indicating that the 43 kDa band was formed by the POG-dependent photoreaction. The 43 kDa band was also immunoreactive to anti-Gβ antibody (Figure 4C, lane 3), and therefore, we concluded that the 43 kDa band represents a cross-linked product of POG-Tγ (8 kDa) with Tβ (35 kDa). No cross-linking was detected between POG-Tγ and soybean trypsin inhibitor (21 kDa protein) which was added to all the samples as a carrier protein in molar excess over POG-T$\beta\gamma$, supporting a specific interaction of the Tγ-bound POG with Tβ. When a mixture of Tα and POG-T$\beta\gamma$ at a molar ratio of 1/1 was subjected to UV irradiation, a new protein band with a molecular mass of 45 kDa was detected by the anti-Tγ antibody which also recognized the Tγ−Tβ adduct (43 kDa) and free Tγ in the same blot (Figure 4A, lane 4). The 45 kDa band was immunoreactive to the anti-Tα antibody (Figure 4B, lane 4), and hence, the 45 kDa band was ascribed to a cross-linked product of POG-Tγ (8 kDa) with Tα (37 kDa).

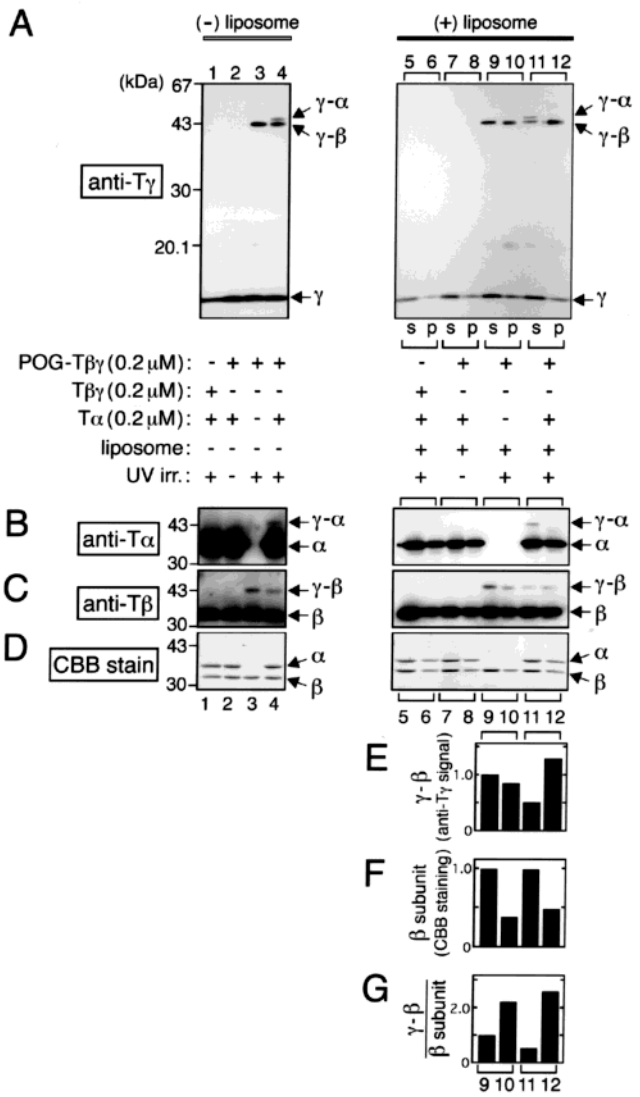

FIGURE 4: Photoaffinity labeling in the presence of liposomes. Each sample (170 μL) contained the indicated combination of 0.2 μM POG-T$\beta\gamma$ or retinal T$\beta\gamma$, 0.2 μM Tα, and liposomes (85 nmol of total lipid) composed of dipalmitoylphosphatidylcholine, 1-palmitoyl-2-oleoylphosphatidylcholine, and cholesterol in a 2/2/1 molar ratio. After UV irradiation, the samples without the liposomes (lanes 1−4) were directly subjected to SDS−polyacrylamide gel (12%) electrophoresis (*37*), whereas those with the liposomes (lanes 5−12) were centrifuged to separate the supernatant (s) and the membrane pellet (p) prior to SDS−PAGE. The proteins were transferred to a PVDF membrane for immunostaining with anti-Tγ (A), anti-Tα (B), or anti-Tβ (C) antibodies. (D) The gel was stained with CBB. (E) The relative levels of Tγ−Tβ cross-linked product (anti-Tγ signals shown in panel A, lanes 9−12) were quantified with digital image processing software, Image Gauge (version 3.45, Fuji Photo Film Co., Ltd.), and were shown in values relative to that of lane 9. (F) The CBB-stained band densities of the Tβ subunit (panel D, lanes 9−12) were quantified and shown in values relative to that of lane 9. (G) The levels of Tγ−Tβ cross-linked product (panel E) were normalized by Tβ protein levels (panel F) to compare the cross-linking efficiencies in the supernatant (lanes 9 and 11) and in the membrane pellet (lanes 10 and 12).

Having characterized the interaction of POG-Tγ with Tα and Tβ in solution, we next conducted the labeling experiments in the presence of the liposomes (Figure 4, lanes 5−12). To examine possible differences in the labeling pattern between POG-T$\beta\gamma$ in solution and its liposome-associated form, the UV-irradiated samples were centrifuged to separate the two forms prior to the immunoblot analyses.

Under these conditions, both the supernatant and the liposome pellet contained POG-T$\beta\gamma$ (Figure 4D). The UV irradiation of the mixture containing the liposomes yielded a Tγ−Tβ adduct not only in the soluble T$\beta\gamma$ (Figure 4A, lane 9) but also in the liposome-associated form (lane 10). When Tα was added, both the Tγ−Tβ and Tγ−Tα cross-linked products were observed in the supernatant following UV irradiation (Figure 4, lane 11), as observed in the absence of the liposomes (Figure 2, lane 4). However, under these conditions, the Tγ−Tα adduct was not detected in the liposome pellet, whereas the Tγ−Tβ adduct was found in both the supernatant and the pellet (Figure 4, lanes 11 and 12). Here, we noticed a clear difference in efficiency of the Tγ−Tβ cross-linking reaction between the supernatant (lanes 9 and 11) and the pellet (lanes 10 and 12). The signal intensities of the Tγ−Tβ adduct (detected with the anti-Tγ antibody; Figure 4A, lanes 9−12) were quantified (Figure 4E), and they were normalized by the band densities of the Tβ subunit stained with Coomassie Brilliant Blue (Figure 4F). The calculated values (Figure 4G) in the pellet (lanes 10 and 12) were 2.2−2.6-fold greater than those in the supernatant (Figure 4G, lanes 9 and 11) in the absence (Figure 4G, lanes 9 and 10) and presence (Figure 4G, lanes 11 and 12) of Tα. This indicates a higher efficiency of the Tγ−Tβ cross-linking reaction in the liposomes than in solution, and suggests a conformational change of Tβ and/or Tγ, including the attached POG upon membrane association of T$\beta\gamma$ and the Tα−T$\beta\gamma$ heterotrimer. On the other hand, no cross-linking of POG-Tγ with a lipid component (see below) was detected in the pellet fraction.

Photoaffinity Labeling of POG-T$\beta\gamma$ in the Presence of Activated Rhodopsin. To gain insight into the role of the C-terminal modification in receptor−G-protein coupling, the molecular interactions of POG were studied in the presence of light-activated rhodopsin. To this end, peripheral proteins, including transducin, were removed from ROS membranes by washing them with a hypotonic buffer (see Experimental Procedures), and the transducin-depleted ROS membranes were exposed to visible (orange) light for formation of the active intermediate of rhodopsin, Rh* (metarhodopsin II). UV irradiation of POG-T$\beta\gamma$ in the presence of the Rh*-containing membranes yielded the 43 kDa Tγ−Tβ cross-linked product that was distributed in both the soluble and membrane fractions (Figure 5A, top panel, lanes 1 and 2). As observed in the presence of the liposomes (Figure 4), Tγ and Tβ were cross-linked more efficiently in the membrane-associated form than in the soluble form (in Figure 5A, compare lanes 1 and 2). Also, addition of Tα-GDP induced the Tγ−Tα cross-link only in the supernatant fraction (Figure 5A, top panel, lane 3). This cross-linked species disappeared when 10 μM GTPγS was added (lane 5), indicating a specific interaction of the C-terminus of Tγ with Tα in the GDP-bound form in the aqueous phase.

In addition to the high-molecular mass cross-linked products described above, UV irradiation of the sample containing Tα-GDP, POG-T$\beta\gamma$, and Rh* in ROS membranes yielded an anti-Tγ immunoreactive low-molecular mass band, termed Tγ−X, that exhibited a mobility slightly slower than that of free Tγ (Figure 5A, middle panel, lane 4). The formation of the Tγ−X adduct was observed only in the membranes (lanes 3 and 4), was strictly dependent on the presence of Tα-GDP (Figure 5A, lanes 2 and 4), and was

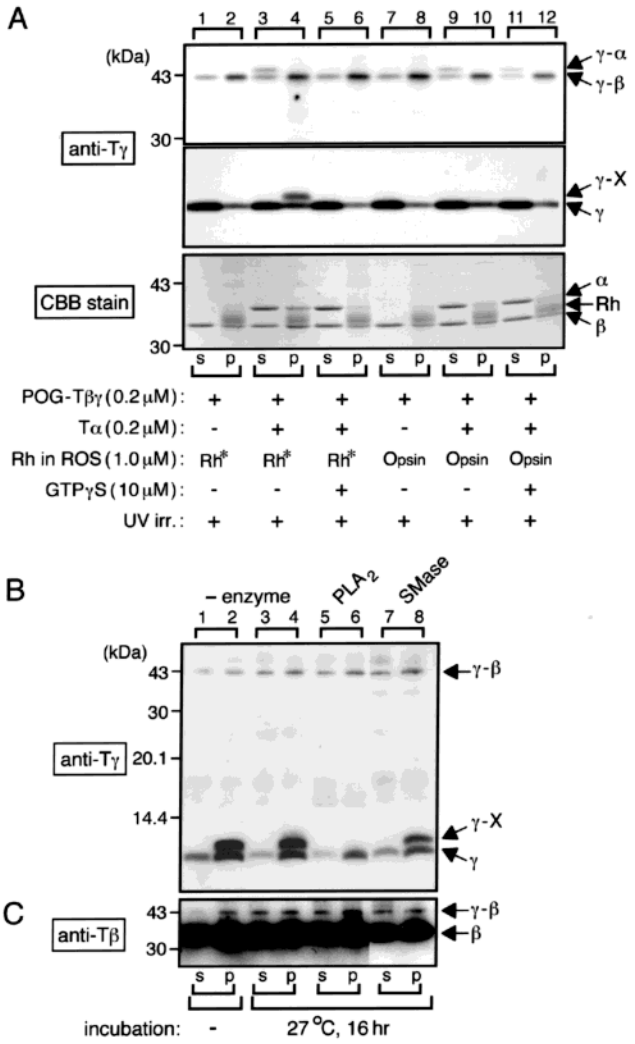

FIGURE 5: Photoaffinity labeling in the presence of Rh* and characterization of the Tγ−X adduct. (A) Each sample (170 μL) contained the indicated combinations of 0.2 μM POG-T$\beta\gamma$, 0.2 μM Tα, 1.0 μM Rh* (or opsin with retinal oxime) in ROS membranes, and 10 μM GTPγS. After UV irradiation, the samples were centrifuged to obtain the supernatant (s) and the membrane pellet (p), which were subjected to SDS−polyacrylamide gel (15%) electrophoresis (*37*). Proteins were transferred to a PVDF membrane for immunostaining with an anti-Tγ antibody. Shown are the clipped images of the blot in the 30−50 kDa region (top panel), the gel front region (middle), and the CBB-stained gel (bottom). (B and C) Each sample (700 μL) containing 0.2 μM POG-T$\beta\gamma$, 1.2 μM Tα, and 1.7 μM Rh* in ROS membranes was UV-irradiated and centrifuged to separate the supernatant (lanes 1, 3, 5, and 7) and membrane (lanes 2, 4, 6, and 8) fractions. These fractions were then supplemented with 0.005% (v/v) Triton X-100 and incubated at 27 °C for 16 h in the absence (lanes 3 and 4) or presence of 10 units of either bee venom phospholipase A_2 (PLA_2, lanes 5 and 6) or *Bacillus* sphingomyelinase (SMase, lanes 7 and 8). Samples were subjected to SDS−PAGE followed by Western blot analysis by using anti-Tγ (B) and anti-Tβ (C) antibodies. Treatment with snake venom (*Naja naja*, from Sigma) PLA_2 gave results similar to those in lanes 5 and 6.

abolished completely by the addition of 10 μM GTPγS (Figure 5A, lane 6). The Tγ−X cross-link was eliminated when Rh*-containing membranes were replaced with opsin membranes (lane 10), in which the photobleaching meta-intermediates had been converted to inactive opsin which was incapable of forming a ternary complex with Tα-GDP and T$\beta\gamma$ (*34*). Together, these results indicate that the cross-link between POG-Tγ and X is dependent on formation of

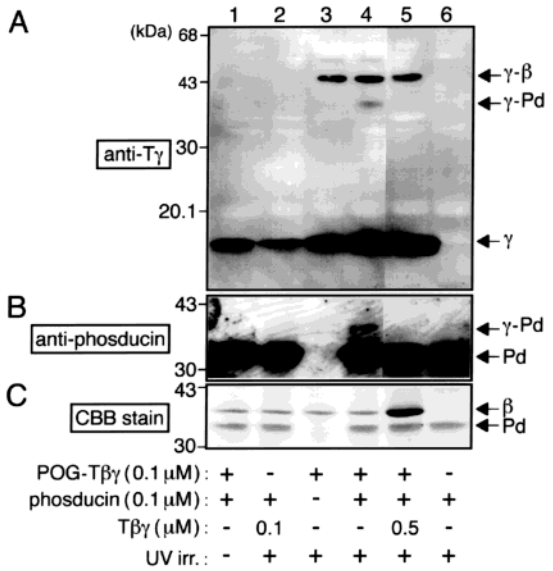

FIGURE 6: Photoaffinity labeling in the presence of phosducin. Each sample (150 μL) contained the indicated combinations of 0.1 μM POG-T$\beta\gamma$, 0.1 μM phosducin, and retinal T$\beta\gamma$ (0.1 or 0.5 μM). After UV irradiation, the samples were subjected to SDS−polyacrylamide gel (12%) electrophoresis (*36*) and Western blot analysis by using anti-Tγ (A) and anti-phosducin (B) antibodies. (C) The gel was stained with CBB.

the ternary complex (Rh*−Tα-GDP−T$\beta\gamma$) in the membrane.

The membrane localization of the Tγ−X adduct suggested that X might be a lipid molecule. To address this possibility, the UV-irradiated sample containing the Tγ−X adduct was treated with phospholipase A_2 (PLA_2). The PLA_2 treatment resulted in the disappearance of the Tγ−X band (Figure 5B, lane 6), whereas sphingomyelinase (SMase) treatment induced no significant change in the intensity of the Tγ−X band relative to that of free Tγ (Figure 5B, lane 8). In contrast, neither PLA_2 nor SMase treatment affected the Tγ−Tβ band (Figure 5B, C). The specific degradation of the Tγ−X adduct by PLA_2 is indicative of X being glycerophospholipid, the most abundant lipid in bovine ROS membranes (*38*, *39*). It is uncertain why no concomitant increase was observed in the blot intensity of free Tγ after PLA_2 treatment (Figure 5, lanes 4 and 6), but it might be due to a difference in the efficiency of blotting to the PVDF membrane between Tγ and the Tγ−X adduct.

Photoaffinity Labeling of POG-T$\beta\gamma$ Complexed with Phosducin. As noted in the introductory section, T$\beta\gamma$ function can also be modulated through interaction with the cytosolic protein phosducin. To investigate whether the C-terminal modification of Tγ is involved in the interaction with phosducin (*25*, *26*, *40*), POG-dependent cross-linking of Tγ was studied in the presence of recombinant phosducin [see Experimental Procedures; the nonphosphorylated form was used in this study because phosphorylated phosducin has a weaker affinity for T$\beta\gamma$ (*6*)]. Gel permeation chromatography analysis confirmed the stable and stoichiometric formation of a complex of recombinant phosducin with POG-T$\beta\gamma$ (ref *10* and data not shown). UV irradiation of the complex of POG-T$\beta\gamma$ and phosducin once again yielded the 43 kDa Tγ−Tβ adduct, and in addition, a distinct 39 kDa band was recognized by the anti-Tγ antibody (Figure 6A, lane 4). This 39 kDa band was also recognized by the anti-phosducin antibody (Figure 6B, lane 4) but not by the anti-Tβ antibody (data not shown), indicating the formation of the Tγ−phosducin cross-link. Since the Tγ−phosducin adduct was no longer detected when a 5-fold molar excess of retinal T$\beta\gamma$ was included in the labeling mixture (Figure 6A, B, lane 5), we concluded that the labeling represents a specific interaction of phosducin with POG linked to Tγ. The simultaneous cross-linking of POG-Tγ with both Tβ and phosducin suggests that the C-terminal modifying lipid of Tγ is located at the interface between Tβ and phosducin in the complex.

DISCUSSION

In the study presented here, we investigated the molecular interactions of the farnesyl moiety of Tγ through a photoaffinity labeling approach utilizing T$\beta\gamma$ modified with POG, a farnesyl analogue that contains a photoreactive azido group at its distal tip. The utility of POG as a farnesyl substitute was demonstrated by the ability of POG-modified T$\beta\gamma$ to support Rh*-catalyzed binding of GTPγS to Tα (Figure 3), an activity of T$\beta\gamma$ that is completely dependent on Tγ lipidation (*10*). In addition, because the elution position of POG-modified Tγ was very close to that of retinal (farnesylated) Tγ in the reverse phase HPLC analysis (Figure 2), the hydrophobicity of POG appears to be very similar to that of farnesyl (*10*, *17*). These properties of POG strengthen the conclusions reached from the cross-linking data obtained in the study presented here, and encourage application of this compound to future analysis of the farnesyl-dependent molecular interactions of the other farnesylated proteins such as Ras (*9*).

Under a variety of experimental conditions, we invariably detected the UV irradiation-dependent cross-link between POG-Tγ and Tβ. Taking into account the position of the photoreactive azido group, we speculate that the distal tip of the farnesyl is located in the vicinity of Tβ rather than being buried deep in the membranes. Such a location of the farnesyl in T$\beta\gamma$ was predicted from the crystal structure of the soluble T$\beta\gamma$−phosducin complex (*26*), which is the only structure ever determined using farnesylated T$\beta\gamma$. Molecular fitting of the electron density map suggested that the tip of the farnesyl is buried in the cavity of the propeller structure of Tβ, although the precise chemical entity accounting for the electron density has not been elucidated (*26*). The results reported here are consistent with this prediction, and provide direct evidence for the functionally important interaction of Tβ with the C-terminal lipid of Tγ even in the membrane. In this regard, it is interesting to note that Gβ1γ2 mutants created with the aim of disrupting the putative prenyl-binding cavity in Gβ1 exhibited impaired G$\beta\gamma$ activity toward the effectors (*41*).

We interpret the finding that the relative level of Tγ−Tβ cross-linking differed between T$\beta\gamma$ in the membrane and the supernatant fractions (Figures 4 and 5), indicating that the mode of farnesyl−Tβ interaction changes upon membrane association of T$\beta\gamma$ due the conformational change of Tβ and/or Tγ, including the modifying lipid. On the other hand, no evidence was obtained for interaction of POG with Rh* in this study (Figure 5), although it was shown that farnesylated short peptides corresponding to the C-terminal region of Tγ interacted directly with Rh* (*42* -*44*). The absence of POG-mediated cross-linking of Tγ with Rh*

(Figure 5) is unlikely due to the lack of Tγ methylation, a modification that has not been addressed in the current study, because the preceding studies also utilized nonmethylated forms of the farnesylated peptides (*42*−*44*). Previously, we demonstrated that the nonmethylated form of farnesylated T$\beta\gamma$ can promote the GDP−GTP exchange reaction on Tα catalyzed by Rh* at an efficiency slightly lower than that of fully modified T$\beta\gamma$ (*34*), whereas the methylation of Tγ significantly enhanced membrane association of T$\beta\gamma$ (*34*). Thus, it is intriguing to ask whether the methylation of POG-T$\beta\gamma$ may simply increase the yield of POG-mediated cross-linking reactions observed in this paper. We are currently attempting to extend our studies to include an analysis with the methylated form of POG-T$\beta\gamma$. While this has been technically challenging, we hope to have such a system in place soon.

In addition to the cross-linking of the T$\beta\gamma$ complex, an interaction of the farnesyl with Tα-GDP was indicated by the cross-linking of this subunit with POG-Tγ in the aqueous phase (Figures 4 and 5). The Tγ−Tα cross-linked product was not detected in the membranes, suggesting the possibility that the interaction of the farnesyl moiety with Tα occurs in the aqueous phase to recruit Tα to T$\beta\gamma$ for formation of the Tα−T$\beta\gamma$ heterotrimer. Synthetic farnesylated peptides corresponding to the C-terminal region of Tγ (*18*) and farnesyl thiosalicylate derivatives (*45*) inhibited formation of the Tα−T$\beta\gamma$ heterotrimer in the aqueous phase in a competitive and reversible manner, suggesting a farnesyl-binding site on Tα. The POG-mediated cross-linking of Tγ with Tα in the aqueous phase may be consistent with the existence of such a putative farnesyl-interacting site on Tα. Interestingly, this interaction appears to be disrupted upon the membrane association of the Tα−T$\beta\gamma$ heterotrimer (Figures 4 and 5), suggesting a "switch" in the farnesyl moiety that results in it now playing a role in stabilizing the membrane binding of transducin (discussed below). Yet another possibility that has not been ruled out is that the farnesyl moiety of Tγ interacts with Tα in the membranes, and that the Tγ−Tα cross-linking destabilized the membrane association of the Tα−T$\beta\gamma$ heterotrimer.

In support of the functional switchover of the modifying lipid, the POG moiety in POG-Tγ interacted with a glycerophospholipid only when POG-T$\beta\gamma$ associated with Tα-GDP and Rh* in ROS membranes (Figure 5). The Tγ−phospholipid cross-linking required the active conformation of rhodopsin (Figure 5A), and the cross-link was abolished completely by the addition of GTPγS under the conditions known to disrupt the Tα−T$\beta\gamma$−Rh* ternary complex. These results clearly indicate a unique conformation of the farnesyl in the large complex that is important for the G-protein-mediated signaling. It is likely that the distal tip of POG moves from the cavity in Tβ toward the membranes upon formation of the ternary complex. It is also possible, however, that POG still remains in the Tβ cavity and simultaneously interacts with the membrane lipid. For example, a global turnover of the POG group or a local rotation at its tip portion in the Tβ cleft may similarly account for the observed cross-linking pattern if one assumes the hydrophobic cleft of Tβ to be exposed to the membranes. Regardless of such a distinction, we would emphasize that our data indicate that the formation of the ternary complex, an important assembly for the G-protein signaling, is accompanied by a local conformational change in the vicinity of the farnesyl (Figure 5); such a conformational change has never before been demonstrated directly.

In the prevailing model of membrane association, the prenyl group linked to a variety of heterotrimeric and monomeric G-proteins is postulated to be inserted into the lipid bilayer to serve as a static membrane anchor. Several lines of evidence do support the idea that the prenyl group plays a direct role in membrane binding. For example, the membrane binding of recombinant T$\beta\gamma$ was markedly augmented by replacing the farnesyl group with the more hydrophobic geranylgeranyl group (*19*). It is interesting to note that a farnesylated short peptide derived from the C-terminal sequence of N-Ras binds to and dissociates from membranes with a rapid turnover rate (*46*). In contrast, the results reported here indicate that the distal tip of POG interacts with the membrane lipid only transiently and specifically in terms of the signaling state of transducin, and the membrane association of T$\beta\gamma$ may not always be accompanied by the insertion of the farnesyl moiety into the membranes. It seems most conceivable that the farnesyl moiety interacts with the membranes with its tip in the vicinity of Tβ, thereby conferring a "sticky" domain on T$\beta\gamma$. In a model for the receptor-catalyzed GDP−GTP exchange reaction on Gα, the activated receptor is supposed to tilt G$\beta\gamma$ in its position toward Gα and thereby uses G$\beta\gamma$ as a lever to pull open the lip of the nucleotide-binding pocket of Gα for promotion of the GDP−GTP exchange reaction ("lever hypothesis") (*47*). It is intriguing to speculate that the sticky domain on T$\beta\gamma$ might serve as a fulcrum of the lever in the transducin−Rh* complex.

The photoaffinity labeling experiments with phosducin in solution yielded a relatively small amount of the Tγ−phosducin cross-linked product in addition to a level of the Tγ−Tβ adduct that was indistinguishable from that observed in the absence of phosducin (Figure 6, lanes 3 and 4). This finding suggests that the distal tip of POG is located at the interface between Tβ and phosducin in a position that enables POG to interact with the two proteins simultaneously, even though the crystallographic analysis predicts that farnesyl is more buried in Tβ (*26*). We believe that the POG moiety in Tγ might exist in an equilibrium of positions in the vicinity of both Tβ and phosducin. In any event, it seems likely that phosducin binding masks the hydrophobic farnesyl-harboring domain of T$\beta\gamma$ (*26*), thereby facilitating dissociation of T$\beta\gamma$ from membranes. Interestingly, a similar mode of prenyl-dependent interaction was reported in the Cdc42−RhoGDI complex. Like the action of phosducin on T$\beta\gamma$, the association of RhoGDI with Cdc42, a geranylgeranylated small G-protein, results in translocation of Cdc42 from the membranes to the cytosol. However, despite the parallels between the two complexes, in the Cdc42−RhoGDI complex the geranylgeranyl group of Cdc42 inserts deeply into the RhoGDI molecule without an interaction with Cdc42 itself (*48*). It is likely that the farnesyl group of T$\beta\gamma$ provides an interaction at a molecular interface looser than that typically observed with the geranylgeranyl group, or alternatively that the two types of isoprenyl groups, farnesyl and geranylgeranyl, might provide significantly divergent modes of protein−protein and protein−membrane interactions. In another example of prenyl-mediated protein−protein interactions, the interaction of Gβ1γ2 with its effector, phospho-

lipase Cβ, was facilitated by a direct interaction of the geranylgeranyl group with the effector rather than with membranes (*49*). It was also reported that the stable association of H-Ras with either the Raf-1 cystein-rich domain (*50*) or phosphoinositide 3-kinase p110γ (*51*) required farnesylation of H-Ras, and further processing (aaX cleavage and/or methylation) of the C-terminus was not essential for these interactions (*50*, *51*). Interestingly, the binding domain(s) for binding of H-Ras to p110γ does not include the farnesyl group, and the binding to p110γ appears to induce a conformational change in farnesylated H-Ras, thereby increasing the affinity for p110γ (*51*). Thus, the modes of prenyl-mediated protein interaction may vary remarkably among prenylated proteins.

In conclusion, the distal tip of the farnesyl mimic POG linked to Tγ interacts with Tβ even in the membrane-associated form, making it unlikely that the prenyl group serves simply as a static membrane anchor. The modifying lipid does also interact with membrane lipids when transducin couples to activated rhodopsin, but this appears to be a very transient interaction. This study provides a valuable insight into the detailed molecular mechanisms underlying signal transduction mediated through G-proteins.

ACKNOWLEDGMENT

We thank Dr. Takahiko Matsuda (The University of Tokyo) for Tβ and Tγ baculoviruses and Dr. Takuhiro Ito (The University of Tokyo) for NMR spectroscopy. We also thank Mr. Yuichi Hashimoto in our laboratory for his critical comments.

SUPPORTING INFORMATION AVAILABLE

A Western blot obtained by the photoaffinity cross-linking experiment using DATFP-geranyl T$\beta\gamma$. This material is available free of charge via the Internet at http://pubs.acs.org.

REFERENCES

1. Gilman, A. G. (1987) G proteins: Transducers of receptor-generated signals, *Annu. Rev. Biochem. 56*, 615−649.
2. Hamm, H. E. (1998) The many faces of G protein signaling, *J. Biol. Chem. 273*, 669−672.
3. Fukada, Y., and Yoshizawa, T. (1981) Activation of phosphodiesterase in frog rod outer segment by an intermediate of rhodopsin photolysis, *Biochim. Biophys. Acta 675*, 195−200.
4. Lee, R. H., Lieberman, B. S., and Lolley, R. N. (1987) A novel complex from bovine visual cells of a 33000-dalton phosphoprotein with β- and γ-transducin: Purification and subunit structure, *Biochemistry 26*, 3983−3990.
5. Kuo, C. H., Akiyama, M., and Miki, N. (1989) Isolation of a novel retina-specific clone (MEKA cDNA) encoding a photoreceptor soluble protein, *Brain Res. Mol. Brain Res. 6*, 1−10.
6. Yoshida, T., Willardson, B. M., Wilkins, J. F., Jensen, G. J., Thornton, B. D., and Bitensky, M. W. (1994) The phosphorylation state of phosducin determines its ability to block transducin subunit interactions and inhibit transducin binding to activated rhodopsin, *J. Biol. Chem. 269*, 24050−24057.
7. Fukada, Y., Takao, T., Ohguro, H., Yoshizawa, T., Akino, T., and Shimonishi, Y. (1990) Farnesylated γ-subunit of photoreceptor G protein indispensable for GTP-binding, *Nature 346*, 658−660.
8. Lai, R. K., Perez-Sala, D., Canada, F. J., and Rando, R. R. (1990) The γ subunit of transducin is farnesylated, *Proc. Natl. Acad. Sci. U.S.A. 87*, 7673−7677.
9. Zhang, F. L., and Casey, P. J. (1996) Protein prenylation: Molecular mechanisms and functional consequences, *Annu. Rev. Biochem. 65*, 241−269.
10. Matsuda, T., and Fukada, Y. (2000) Functional analysis of farnesylation and methylation of transducin, *Methods Enzymol. 316*, 465−481.
11. Boyartchuk, V. L., Ashby, M. N., and Rine, J. (1997) Modulation of Ras and a-factor functions by calboxyl-terminal proteolysis, *Science 275*, 1796−1800.
12. Jang, G. F., and Gelb, M. H. (1998) Substrate specificity of mammalian prenyl protein-specific endoprotease activity. *Biochemistry 37*, 4473−4481.
13. Otto, J. C., Kim, E., Young, S. G., and Casey, P. J. (1999) Cloning and characterization of a mammalian prenyl protein-specific protease, *J. Biol. Chem. 274*, 8379−8382.
14. Bergo, M. O., Leung, G. K., Ambroziak, P., Otto, J. C., Casey, P. J., Gomes, A. Q., Seabra, M. C., and Young, S. G. (2001) Isoprenylcysteine carboxyl methyltransferase deficiency in mice, *J. Biol. Chem. 276*, 5841−5845.
15. Fukada, Y., Ohguro, H., Saito, T., Yoshizawa, T., and Akino, T. (1989) $\beta\gamma$-Subunits of bovine transducin composed of two components with distinctive γ-subunits, *J. Biol. Chem. 264*, 5937−5943.
16. Ohguro, H., Fukada, Y., Yoshizawa, T., Saito, T., and Akino, T. (1990) A specific $\beta\gamma$-subunit of transducin stimulates ADP-ribosylation of the α-subunit by pertussis toxin, *Biochem. Biophys. Res. Commun. 167*, 1235−1241.
17. Ohguro, H., Fukada, Y., Takao, T., Shimonishi, Y., Yoshizawa, T., and Akino, T. (1991) Carboxyl methylation and farnesylation of transducin γ-subunit synergistically enhance its coupling with metarhodopsin II, *EMBO J. 10*, 3669−3674.
18. Matsuda, T., Takao, T., Shimonishi, Y., Murata, M., Asano, T., Yoshizawa, T., and Fukada, Y. (1994) Characterization of interactions between transducin α/$\beta\gamma$-subunits and lipid membranes, *J. Biol. Chem. 269*, 30358−30363.
19. Matsuda, T., Hashimoto, Y., Ueda, H., Asano, T., Matsuura, Y., Doi, T., Takao, T., Shimonishi, Y., and Fukada, Y. (1998) Specific isoprenyl group linked to transducin γ-subunit is a determinant of its unique signaling properties among G-proteins, *Biochemistry 37*, 9843−9850.
20. Higgins, J. B., and Casey, P. J. (1996) The role of prenylation in G-protein assembly and function, *Cell. Signal. 8*, 433−437.
21. Fu, H. W., and Casey, P. J. (1999) Enzymology and biology of CaaX protein prenylation, *Recent Prog. Horm. Res. 54*, 315−343.
22. Wall, M. A., Coleman, D. E., Lee, E., Iñiguez-Lluhi, J. A., Posner, B. A., Gilman, A. G., and Sprang, S. R. (1995) The structure of the G protein heterotrimer G$i\alpha_1\beta_1\gamma_2$, *Cell 83*, 1047−1058.
23. Lambright, D. G., Sondek, J., Bohm, A., Skiba, N. P., Hamm, H. E., and Sigler, P. B. (1996) The 2.0 Å crystal structure of a heterotrimeric G protein, *Nature 379*, 311−319.
24. Sondek, J., Bohm, A., Lambright, D. G., Hamm, H. E., and Sigler, P. B. (1996) Crystal structure of a G_A protein $\beta\gamma$ dimer at 2.1 Å resolution, *Nature 379*, 369−374.
25. Gaudet, R., Bohm, A., and Sigler, P. B. (1996) Crystal structure at 2.4 Å resolution of the complex of transducin $\beta\gamma$ and its regulator, phosducin, *Cell 87*, 577−588.
26. Loew, A., Ho, Y. K., Blundell, T., and Bax, B. (1998) Phosducin induces a structural change in transducin $\beta\gamma$, *Structure 6*, 1007−1019.
27. Kawata, A., Oishi, T., Fukada, Y., Shichida, Y., and Yoshizawa, T. (1992) Photoreceptor cell types in the retina of various vertebrate species: Immunocytochemistry with antibodies against rhodopsin and iodopsin, *Photochem. Photobiol. 56*, 1157−1166.
28. Baba, T., and Allen, C. M. (1984) Inactivation of undecaprenylpyrophosphate synthetase with a photolabile analogue of farnesyl pyrophosphate, *Biochemistry 23*, 1312−1322.
29. Davisson, V. J., Woodside, A. B., Neal, T. R., Stremler, K. E., Muehlbacher, M., and Poulter, C. D. (1986) Phosphorylation of isoprenoid alcohols, *J. Org. Chem. 51*, 4768−4779.
30. Shi, G., and Xu, Y. (1990) Trifluoromethyl-substituted carbethoxy carbene as a novel CF_3-containing a2 synthon equivalent for the preparation of 2-(trifluoromethyl)-4-oxo carboxylic ester derivatives: highly functionalized synthetic building blocks bearing a CF_3 group, *J. Org. Chem. 55*, 3383−3386.
31. Caplin, B. E., Ohya, Y., and Marshall, M. S. (1998) Amino acid residues that define both the isoprenoid and C*AAX* preferences of the *Saccharomyces cerevisiae* protein farnesyltransferase, *J. Biol. Chem. 273*, 9472−9479.

32. Chen, W. J., Moomaw, J. F., Overton, L., Kost, T. A., and Casey, P. J. (1993) High level expression of mammalian protein farnesyltransferase in a baculovirus system, *J. Biol. Chem. 268*, 9675−9680.
33. Moomaw, J. F., Zhang, F. L., and Casey, P. J. (1995) Isolation of protein prenyltransferase from bovine brain and baculovirus expression system, *Methods Enzymol. 250*, 12−21.
34. Fukada, Y., Matsuda, T., Kokame, K., Takao, T., Shimonishi, Y., Akino, T., and Yoshizawa, T. (1994) Effects of carboxyl methylation of photoreceptor G protein γ-subunit in visual transduction, *J. Biol. Chem. 269*, 5163−5170.
35. Bangham, A. D., Standish, M. M., and Watkins, J. C. (1965) Diffusion of univalent ions across the lamellae of swollen phospholipids, *J. Mol. Biol. 13*, 238−252.
36. Laemmli, U. K. (1970) Cleavage of structural proteins during the assembly of the head of bacteriophage T4, *Nature 227*, 680−685.
37. Ausubel, F. M., Brent, R., Kingston, R. E., Moore, D. D., Seidman, J. G., Smith, J. A., and Struhl, K. (1995) *Short Protocols in Molecular Biology*, 3rd ed., Chapter 10, pp 13−14, John Wiley & Sons, Hoboken, NJ.
38. Borggreven, J. M. P. M., Daemen, F. J. M., and Bonting, S. L. (1970) Biochemical aspects of the visual process. The lipid composition of native and hexane-extracted cattle rod outer segments, *Biochim. Biophys. Acta 202*, 374−381.
39. Shichi, H. (1971) Biochemistry of visual pigments. Phospholipid requirement and opsin conformation for regeneration of bovine rhodopsin, *J. Biol. Chem. 246*, 6178−6182.
40. Tanaka, H., Kuo, C. H., Matsuda, T., Fukada, Y., Hayashi, F., Ding, Y., Irie, Y., and Miki, N. (1996) MEKA/Phosducin attenuates hydrophobicity of transducin $\beta\gamma$ subunits without binding to farnesyl moiety, *Biochem. Biophys. Res. Commun. 223*, 587−591.
41. Myung, C. S., and Garrison, J. C. (2000) Role of C-terminal domains of the G protein β subunit in the activation of effectors, *Proc. Natl. Acad. Sci. U.S.A. 97*, 9311−9316.
42. Kisselev, O., Ermolaeva, M., and Gautam, N. (1995) Efficient interaction with a receptor requires a specific type of prenyl group on the G protein γ subunit, *J. Biol. Chem. 270*, 25356−25358.
43. McCarthy, N. E. M., and Akhtar, M. (2000) Function of the farnesyl moiety in visual signaling, *Biochem. J. 347*, 163−171.
44. Bartl, F., Ritter, E., and Hofmann, K. P. (2000) FTIR spectroscopy of complexes formed between metarhodopsin II and C-terminal peptides from the G-protein α- and γ-subunits, *FEBS Lett. 473*, 259−264.
45. Dietrich, A., Scheer, A., Illenberger, D., Kloog, Y., Henis, Y. I., and Gierschik, P. (2003) Studies on G protein $\alpha\beta\gamma$ heterotrimer formation reveal a putative S-prenyl binding site in the α subunit, *Biochem. J. 376*, 449−456.
46. Schroeder, H., Leventis, R., Rex, S., Schelhaas, M., Nägele, E., Waldmann, H., and Silvius, J. R. (1997) S-Acylation and plasma membrane targeting of the farnesylated carboxy-terminal peptide of N-*ras* in mammalian fibroblasts, *Biochemistry 36*, 13102−13109.
47. Rondard, P., Iiri, T., Srinivasan, S., Meng, E., Fujita, T., and Bourne, H. R. (2001) Mutant G protein α subunit activated by G$\beta\gamma$: A model for receptor activation? *Proc. Natl. Acad. Sci. U.S.A. 98*, 6150−6155.
48. Hoffman, G. R., Nassar, N., and Cerione, R. A. (2000) Structure of Rho family GTP-binding protein Cdc42 in complex with the multifunctional regulator RhoGDI, *Cell 100*, 345−356.
49. Fogg, V. C., Azpiazu, I., Linder, M. E., Smrcka, A., Scarlata, S., and Gautam, N. (2001) Role of the γ subunit prenyl moiety in G protein $\beta\gamma$ complex interaction with phospholipase Cβ, *J. Biol. Chem. 276*, 41797−41802.
50. Williams, J. G., Drugan, J. K., Yi, G.-S., Clark, G. J., Der, C. J., and Campbell, S. L. (2000) Elucidation of the binding determinants and functional consequences of Ras/Raf-cysteine-rich domain interactions, *J. Biol. Chem. 275*, 22172−22179.
51. Rubio, I., Wittig, U., Meyer, C., Heinze, R., Kadereit, D., Waldmann, H., Downward, J., and Wetzker, R. (1999) Farnesylation of Ras is important for the interaction with phosphoinositide 3-kinase γ, *Eur. J. Biochem. 266*, 70−82.

BI0351514